ACS APPLIED MATERIALS & INTERFACES

Research Article

www.acsami.org

Decreased Aperture Surface Energy Enhances Electrical, Mechanical, and Temporal Stability of Suspended Lipid Membranes

Leonard K. Bright,[†] Christopher A. Baker,[†] Mark T. Agasid,[†] Lin Ma,[†] and Craig A. Aspinwall*[,†,‡]

[†]Department of Chemistry and Biochemistry and [‡]BIO5 Institute, University of Arizona, Tucson, Arizona 85721, United States

Supporting Information

ABSTRACT: The development of next-generation transmembrane protein-based biosensors relies heavily on the use of black lipid membranes (BLMs); however, electrical, mechanical, and temporal instability of BLMs poses a limiting challenge to biosensor development. In this work, micrometer-sized glass apertures were modified with silanes of different chain length and fluorine composition, including 3-cyanopropyldimethychlorosilane (CPDCS), ethyldimethylchlorosilane (EDCS), *n*-octyldimethylchlorosilane (ODCS), (tridecafluoro-1, 1, 2, 2-tetrahydrooctyl)dimethylchlorosilane (PFDCS), or (heptadecafluoro-1,1,2,2-tetrahydrodecyl)dimethylchlorosilane (PFDDCS), to explore the effect of substrate surface energy on BLM stability. Low energy silane-modified surfaces promoted enhanced lipid−substrate interactions that facilitate the formation of low-leakage, stable BLMs. The surface energies of silane-modified substrates were 30 ± 3, 16 ± 1, 14 ± 2, 11 ± 1, and 7.1 ± 2 mJ m^{-2} for CDCS, EDCS, ODCS, PFDCS, and PFDDCS, respectively. Decreased surface energy directly correlated to improved electrical, mechanical, and temporal BLM stability. Amphiphobic perfluorinated surface modifiers yielded superior performance compared to traditional hydrocarbon modifiers in terms of stability and BLM formation, with only marginal effects on BLM membrane permeability. Leakage currents obtained for PFDCS and PFDDCS BLMs were elevated only 10−30%, though PFDDCS modification yielded >5-fold increase in electrical stability as indicated by breakdown voltage (> 2000 mV vs 418 ± 73 mV), and >25-fold increase in mechanical stability as indicated by air−water transfers (> 50 vs 2 ± 0.2) when compared to previously reported CPDCS modification. Importantly, the dramatically improved membrane stabilities were achieved with no deleterious effects on reconstituted ion channel function, as evidenced by α-hemolysin activity. Thus, this approach provides a simple, low cost, and broadly applicable alternative for BLM stabilization and should contribute significantly toward the development of next-generation ion-channel-functionalized biosensors.

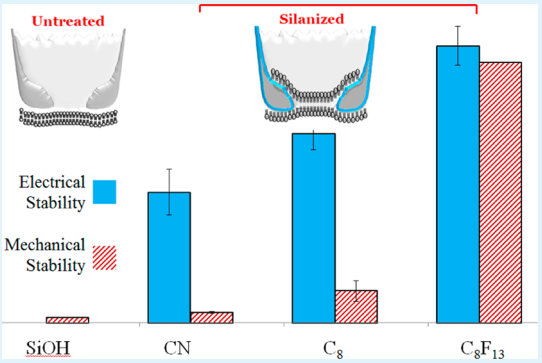

KEYWORDS: *black lipid membrane, aperture, membrane stability, silane-modified surface, surface energy*

INTRODUCTION

Ion channels transport ions across biological membranes in a ligand, voltage, and/or ion concentration-dependent manner. Ion channels are potentially powerful transducers for high sensitivity, label-free chemical measurements because small changes in ion flux across phospholipid membranes can be measured electrically with high sensitivity. Ion channels are increasingly used for nucleic acid sequencing[1−3] and genotyping,[4,5] and have been used to detect electrochemically and optically inactive analytes,[6] divalent metal ions,[7] drugs,[8] pesticides, and other compounds.[9,10] The most common implementations of ion channel measurement for sensing and sequencing involve the reconstitution of ion channels into an artificial lipid bilayer suspended across a microaperture, commonly referred to as a black lipid membrane (BLM).[11] A key limitation in the continued development of ion-channel-functionalized sensors remains the ability to form BLMs with sufficient electrical, temporal, and mechanical stability in a manner that is broadly applicable.[12,13] Methods that overcome these challenges in a manner that is accessible to researchers across multiple disciplines will significantly enable the development of next-generation ion-channel-functionalized biosensors. A number of mechanisms for BLM stabilization have been developed, including, but not limited to, integration of stabilizing polymer layers at the BLM interface, the use of reactive lipids, and reduction of aperture size.

Stability can be improved by sandwiching the bilayer between gel phase materials or viscous polymers.[14−16] While this approach is very powerful for nanopore sequencing and static sensor measurements, time-resolved sensing is limited because viscous polymers inhibit diffusional access of analytes in solution to the ion channel, thus increasing response times.

Increased BLM stability has been achieved using synthetic lipids via photopolymerization of reactive lipids.[17−21] While polymerized BLMs offer unparalleled stability, their use is complicated by decreased membrane fluidity, which is required

Received: August 28, 2013
Accepted: November 4, 2013
Published: November 4, 2013

for ion channel insertion and activity.[18,20] Further, synthetic polymerizable lipids are costly to produce and few are commercially available, significantly limiting the widespread adoption of this approach.[22,23] To accelerate widespread sensor development, more robust and readily available methods are required for BLM stabilization.

Methods that improve BLM stability by decreasing the size or modifying the surface chemistry of the aperture show promise because BLM function is not affected. Stable supported bilayers have been formed on hydrophilic glass substrates containing nm-sized apertures in which the lipid head groups interact with the glass surface (Figure 1A).[24] While

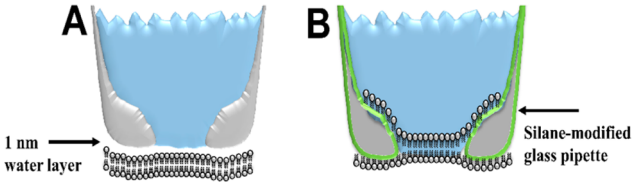

Figure 1. Schematic of BLM formation on unmodified and silane-modified glass microapertures. (A) Unmodified micropipet apertures yield supported lipid bilayers with a conductive water layer approximately 1 nm thick. (B) Silane-modified micropipet apertures result in suspended lipid bilayers with a tails-down lipid orientation at the lipid–glass interface.

the stability is markedly increased compared to micrometer-sized apertures, primarily due to the reduced surface area of the BLM, the corresponding decrease in surface area complicates aperture fabrication and bilayer formation. The low nm aperture diameters also require extended time and ion channel concentrations to achieve active sensors. Furthermore, this approach suffers from elevated conductance via ion leakage through the ca. 1 nm H_2O layer between the hydrophilic glass surface and the polar lipid head groups (Figure 1A) due to enhanced radial migration via the confined water layer upon voltage application,[25] potentially limiting the sensitivity of ion-channel-functionalized sensors.

To overcome this limitation, nm- and μm-sized apertures fabricated in glass pipettes have been modified with 3-cyanopropyldimethyl-chlorosilane (CPDCS), which forms a self-assembled monolayer that decreases the energy of the glass surface.[18,26,27] Decreased surface energy facilitates lipid monolayer formation by promoting interactions between the hydrophobic lipid tail and the aperture substrate material,[28,29] similar to that observed on large Teflon apertures.[30] On CPDCS-modified surfaces, BLMs form when lipid monolayers join from opposite faces of a pipette aperture to form a suspended bilayer (Figure 1B)[26,31] analogous to the Montal–Mueller technique of folding two lipid monolayers from opposite sides of a Teflon aperture.[32,33] While CPDCS modification has proven useful in the formation of low leakage BLMs on glass apertures,[18] the temporal and mechanical stability for μm-sized apertures using non-polymerizable lipids desirable for sensor and sequencing experiments is still insufficient to catalyze widespread sensor development.[18,31]

To address this key limitation in ion-channel-functionalized sensor development, we explored the effect of the surface energy of the underlying aperture substrate on the electrical, mechanical, and temporal stabilities of BLMs. Micron-sized glass apertures and surfaces were modified with silanes of varying functionality. Surface characterization of modified planar Si substrates was utilized to identify candidates for aperture modification and subsequent studies of electrical performance and BLM stability. The function of highly stabilized BLMs was evaluated via activity measurements of reconstituted ion channels. The resulting BLM stabilization strategy provides a simple, broadly applicable approach for producing highly stable BLMs that is broadly accessible.

EXPERIMENTAL SECTION

Chemicals and Materials. KCl, 2-[4-(2-hydroxyethyl)piperazin-1-yl]ethanesulfonic acid (HEPES), and α-hemolysin (α-HL) were purchased from Sigma-Aldrich (St. Louis, MO). Ethyldimethylchlorosilane (EDCS), 3-aminopropyldimethylethoxysilane (APDES), *n*-octyldimethylchlorosilane (ODCS), 3,3,3-trifluoropropyldimethylchlorosilane (FPDCS), trimethylchlorosilane (TCS), (tridecafluoro-1,1,2,2-tetrahydrooctyl)trichlorosilane (PFTCS), (tridecafluoro-1,1,2,2-tetrahydrooctyl)dimethylchlorosilane (PFDCS), and (heptadecafluoro-1,1,2,2-tetrahydrodecyl)dimethylchlorosilane (PFDDCS) were purchased from Gelest Inc. (Morrisville, PA). 3-Cyanopropyldimethylchlorosilane (CPDCS) was purchased from TCI America Inc. (Portland, OR). The structures for each silane are shown in the Supporting Information (Scheme SI-1). Na_2HPO_4, KH_2PO_4, anhydrous acetonitrile (ACN), 70% H_2SO_4, 30% H_2O_2, and NaCl were purchased from EMD Chemical Inc. (Gibbstown, NJ). Ethanol was purchased from Decon Laboratories (King of Prussia, PA). 1,2-Diphytanoyl-*sn*-glycero-3-phosphocholine (DPhPC), 1,2-dilauroyl-*sn*-glycero-3-phosphocholine (DLPC) in chloroform, and 1,2-dipalmitoyl-*sn*-glycerol-3-phosphoethanolamine-*N*-lissamine rhodamine B sulfonyl (Rh-DPPE) were purchased from Avanti Polar Lipids Inc. (Alabaster, AL). Microscope cover slides (22 × 22 mm^2) and 100-oriented Si wafers used for surface characterization were purchased from VWR (Radnor, PA) and Wafer World, Inc. (West Palm Beach, FL), respectively. H_2O used for all experiments was obtained from a Barnstead EasyPure UV/UF purifier with a minimum resistivity of 18.3 MΩ cm.

Surface Modification of Planar Substrates. Silane monolayers were deposited on glass and Si planar substrates by a solution phase modification. Prior to silanization, substrates were cleaned either by immersion in piranha solution (5:2 70% H_2SO_4:30% H_2O_2) for 30 min or immersion in 1 M HNO_3 for 30 min, with no significant difference observed between the two cleaning procedures. Following cleaning, substrates were rinsed consecutively with H_2O and acetone, and dried consecutively with compressed Ar and baking at 70 °C for 15–30 min. The substrates were immediately transferred to a 2% (v/v) solution of silane modifiers in solvent. ACN was used as the solvent for CPDCS, FPDCS, TCS, and EDCS surface modifications, while toluene was used for ODCS, PFTCS, PFDCS, and PFDDCS modifications. The reaction was allowed to proceed at room temperature with <20% relative humidity for 6–8 h. Reactions that exceeded 8 h resulted in silane-aggregate formation observed by AFM, especially for PFDCS modifications (Supporting Information). Following the reaction, substrates were sonicated successively in ACN or toluene, ethanol, and H_2O for 5 min each and dried with compressed N_2. Static H_2O contact angles, AFM surface scans, and ellipsometry measurements were obtained within 30 min after substrate modification.

Surface Characterization by Atomic Force Microscopy (AFM). An Agilent 5500 AFM (Agilent Technologies, Inc., Chandler, AZ) was used in the tapping mode to measure the surface roughness of native and modified SiO_2 (Si/SiO_2) with a NSC14/AIBS scanning probe tuned between 250 and 400 kHz with a force constant of 5.7 N m^{-1}. The standard scanning probe was mounted on a rectangular 3.4 × 1.6 × 0.4 mm^3 Si chip, with a tip height of 20–30 μm, tip radius <10 nm, and cone angle of <40°. A minimum of three samples were imaged with each substrate scanned at a minimum of three sites. The image scan area was 1 μm^2, and the root-mean-square (RMS) surface roughness were calculated using PicoView 6.2 software (Agilent).

Surface Characterization by Ellipsometry. Monolayer thickness on Si substrates was measured using a model 43603-200E

ellipsometer (Rudolph Research, Santa Clara, CA). The native SiO_2 layer on Si substrate (Si/SiO_2) was measured to be 1.9 ± 0.02 nm based on a refractive index of 1.46. A 632.8 nm HeNe laser line was incident on the sample at an angle of 70°.[34]

Contact Angle Measurements. Contact angles on each modified and unmodified planar substrate were measured using the sessile droplet method at four locations for each substrate, and repeated for at least three replicate substrates. 2 μL ofH_2O or *n*-decane droplets were manually deposited onto the surface of the substrates using a micropipet. Images were acquired using a model TM-7CN video camera (Pulnix America, Inc., Sunnyvale, CA), and contact angles were measured with a model DSA 10 MK2 drop shape analysis system (Kruss, Charlotte, NC).[34]

Formation of Planar Lipid Membranes. DLPC doped with 2 mol % Rh-DPPE was rapidly dried using compressed Ar followed by additional vacuum drying for 4 h. Dried lipid/dye mixture was dissolved in PBS buffer (137 mM NaCl, 2.7 mM KCl, 10 mM Na_2HPO_4, and 2 mM KH_2PO_4 at pH 7.4) to a final concentration of 0.5 mg mL^{-1}. Small unilamellar vesicles were formed by ultrasonication using a cup horn attachment (model W-380, Heat Systems-Ultrasonics, Inc., Newtown, CT) for 30 min at 25 °C, or until the solution appeared clear. Incubation of lipid vesicles on planar glass substrates cleaned with piranha was used as the control. Following 4 h of vesicle fusion, the lipid solution was exchanged at least 12 times with 200 μL of PBS buffer to rinse excess lipids from solution. The substrate surface was scratched to provide fluorescence contrast, and rinsed again with buffer to remove floating debris. Lipid bilayers were distinguished from monolayers by comparing the difference in relative fluorescence intensity of the lipid layers.[26,35] The fluorescence images of lipid layers on glass substrates were collected using a Nikon Eclipse TE300 inverted epifluorescence microscope with a 20×/0.13 N.A. objective (Nikon Instrument Inc., Melville, NY) and a Quantix 57 back-illuminated CCD camera (Roper Scientific, Tucson, AZ). Images were captured using MetaVue software (Universal Imaging, Downingtown, PA) and analyzed using ImageJ.[36]

Pipette Aperture Fabrication and Silanization. Borosilicate capillaries (World Precision Instruments, Novato, CA) with O.D. and I.D. of 1.5 and 1.1 mm, respectively, were fabricated into pipettes containing microapertures using a P-97 micropipet puller (Sutter Instruments, Navato, CA) and fire polished with a model MF-900 microforge (Narishige, East Meadow, NY) to produce aperture diameters of 25−35 μm (Figure S1, Supporting Information) for BLM formation. Aperture diameters of 25−35 μm were specifically chosen because BLM formation can easily be distinguished from supported bilayer formation (Figure 1) or clog formation. Fabricated pipettes were filled and submerged in 0.1 M HNO_3 for 30 min followed by rinsing with H_2O. The pipettes were subsequently rinsed with acetone and dried in an oven at 70° C for 15−30 min. The pipettes were immediately filled and submerged in 2% (v/v) solution of silane modifier dissolved in either ACN or toluene (as previously described) for 6−12 h. The resulting modified pipettes were rinsed with either ACN or toluene, followed by ethanol and H_2O.

Following the initial evaluations of PFTCS, monochlorosilanes or monoethoxysilanes were used for substrate modification because they form uniform monolayers on surface silanol groups compared to trichlorosilanes or triethoxysilanes, which freely polymerize to form heterogeneous silane layers.[37,38]

BLM Formation and Characterization. BLMs were formed using a painting method described previously.[18] Briefly, stock lipid solutions were dried using compressed Ar and then placed in a lyophilizer for at least 4 h. Dried lipid was dissolved in *n*-decane to a final concentration of 10 mg mL^{-1}. DPhPC was used for all BLM studies on functionalized pipette apertures. A 3 μL aliquot of lipid solution was applied to the tip of the pipette and dried with N_2. Prior to BLM formation, pipettes were filled with recording buffer containing 1 M KCl and 5 mM HEPES (pH 7.4). The pipette was mounted on the headstage of a patch clamp amplifier (EPC-8 or EPC-10, HEKA Electronics, Bellmore, NY), and 2 μL of lipid solution was applied near the pipette tip after immersion into recording buffer. The lipid solution was swept gently across the aperture using a plastic pipette tip. A 20 Hz square-wave pulse of ±5 mV versus Ag/AgCl was applied across the pipette aperture, and formation of a BLM was indicated by a change in resistance from 10−100 KΩ (for an open pipette) to 1−10 GΩ (for a BLM).

To verify BLM formation, an increasing potential was applied across the membrane from −100 to 1000 mV in 10 mV increments of 50 ms duration, for a total of 110 steps. When pipettes did not return to open resistance after applying 1000 mV, or 2000 mV in the case of BLMs suspended on perfluorinated modified pipette apertures, clean plastic pipette tips were dragged across the aperture to remove excess lipid/decane solution. When failure to observe a BLM continued (i.e., the apertures were clogged), plastic pipette tips were repeatedly swept across the aperture while applying increasing potential (−100 to +1000 or +2000 mV) to clear the aperture. Air−water transfers (AWT), which refers to the number of times a bilayer survives transport across an air−water interface, and BLM conductance were also used to verify BLM formation. To monitor ion channel activity, 2 μL of α-HL (0.5 mg mL^{-1} in recording buffer) was added to 500 μL bath solution while applying +40 mV across the BLM.

Data Analysis and Presentation. All data is presented in the form of mean ± standard deviation. Error bars within the figures represent 1 standard deviation from the mean. A minimum of three replicate measurements on at least three different planar or BLM substrates were collected for each modification.

RESULTS AND DISCUSSION

BLMs prepared on unmodified glass pipette apertures yield an increased conductance and decreased stability compared to those formed on hydrophobic aperture materials, likely due to the difference in membrane organization at the glass−lipid interface (Figure 1).[24,39] While glass micropipets provide a platform to more readily produce smaller apertures, the increased conductance caused by ion leakage via the thin hydration layer limits the overall utility of these apertures for single channel recordings of low conductance ion channels.[24] CPDCS-modified apertures reduce membrane conductance and ion leakage and provide a moderate extension of BLM lifetime compared to bare glass apertures.[18,26] To our knowledge, the effect of aperture surface energy, a key property in determining the assembly of supported lipid membranes, has not been investigated as a tool to increase BLM stability. If effective, this approach would provide a simple, low cost alternative to membrane stabilization that is more broadly accessible compared to existing stabilization methods and should, therefore, markedly accelerate the development of BLM-functionalized sensors. We hypothesized that decreasing surface energy below that achieved by conventional CPDCS modification would enhance the interactions between the lipids and the substrate near the aperture opening, thus improving BLM stability. Additionally, we hypothesized that amphiphobic surface modifications (repellent to both polar and non-polar solvents) would expedite stable BLM formation and lead to more stable BLMs relative to hydrocarbon modifiers by excluding residual organic solvent at the BLM/support interface. To test these hypotheses, we evaluated planar lipid membrane and BLM formation on modified substrates via surface and electrophysiological characterization.

Characterization of Lipid Monolayer Membranes on Planar Substrates. We first evaluated the properties that lead to stable lipid monolayer formation on planar substrates to identify the optimal conditions for pipette and aperture surface modification. To evaluate the formation of uniform silane monolayers on oxidized planar Si/SiO_2 (Si substrates) after silanization, the monolayer thickness and surface roughness were measured. Si substrates exhibited a lower surface

Table 1. Surface Characterization of Silane Monolayers on Si Substrates

surface modification	silane monolayer thickness (nm)	surface roughness RMS (nm)	H_2O contact angle (deg)	*n*-decane contact angle (deg)	surface energy (mJ m^{-2})
Si (as received)		0.10 ± 0.03	34 ± 7	<10	
acid cleaned	0.00	0.16 ± 0.04	<10	<10	73
CPDCS	0.3 ± 0.04	0.33 ± 0.05	74 ± 1	<10	30 ± 3
EDCS	0.5 ± 0.09	0.31 ± 0.1	93 ± 2	<10	16 ± 1
ODCS	0.5 ± 0.03	0.40 ± 0.08	100 ± 3	<10	14 ± 2
PFDCS	0.6 ± 0.08	0.50 ± 0.1	108 ± 2	52 ± 2	11 ± 1
PFDDCS	0.8 ± 0.1	0.68 ± 0.5	113 ± 2	66 ± 3	7.1 ± 2
PFTCS	5.5 ± 2	2.5 ± 0.4	111 ± 3	63 ± 3	7.9 ± 1

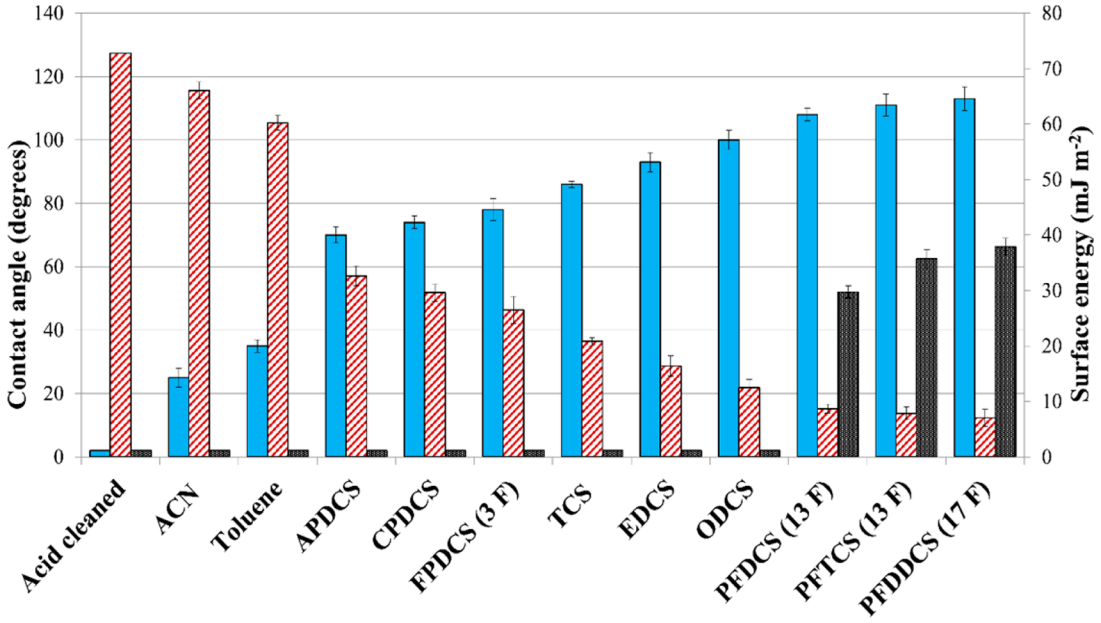

Figure 2. Contact angles and surface energy for planar silane-modified Si surfaces. Water (blue) and *n*-decane (grey) contact angles are indicated by the left *y*-axis. Surface energy (red crosshatch) is indicated by the right *y*-axis.

roughness (RMS = 0.10 nm) than glass substrates (RMS = 0.30 nm), agreeing well with previous reports.[40] Thus, Si substrates were used for subsequent surface characterizations.

Table 1 shows silane surface roughness values, monolayer thicknesses, contact angles, and derived calculated surface energies for the selected modifications. Monolayer thicknesses ranging from 0.3 ± 0.04 to 0.8 ± 0.1 nm were measured using ellipsometry after functionalization with monochlorosilane modifiers, whereas the trichlorosilane modifier (PFTCS) yielded substantial increases in monolayer thickness (Table 1). The measured silane monolayer thickness was observed to increase with increasing hydrophobicity and chain length. Unfortunately, we were unable to characterize the thickness of the hybrid membrane on modified planar surfaces by ellipsometry. Lipid membrane organization is maintained by relatively weak non-covalent interactions that are disrupted upon extended and complete drying, a requisite of our ellipsometry measurments. Prior examination of hybrid membranes prepared from polymerized lipids did provide for ellipsometric measurements, and thicknesses corresponding to a lipid monolayer were observed.[41] Thus, additional surface and membrane characterization was performed.

The roughness of modified surfaces was evaluated, since surface roughness influences surface energy measurements[42] and substantial surface roughness may challenge the formation of BLMs on modified surfaces, or result in BLMs with low resistance electrical seals at the lipid−aperture interface. The RMS roughness calculated from surface area scans of 1 μm^2 was well within the accepted range of <1 nm for BLM and planar supported bilayer formation for all the monochlorosilanes examined, though PFTCS-modified substrates exhibited a RMS roughness of 2.5 ± 0.4 (Table 1). Large aggregates ca. 5−7 nm tall were observed on PFTCS-modified substrates (Supporting Information, Figure S2) due to polymerization of the reactive trichlorosilane functional groups. The formation of a highly polymeric and heterogeneous surface by trichlorosilanes was similar to trialkoxysilanes as previously reported.[38] The thickness of the large aggregates formed by PFTCS-modified substrates correlated with AFM surface roughness, as shown in Table 1. Later studies showed frequent clogging of pipette apertures with PFTCS modifications, thus challenging the formation of BLMs. On PFDCS- and PFDDCS-modified substrates, silane aggregates with diameters of 30−100 nm and ca. 2 nm tall were observed (Supporting Information, Figure S2), although later studies revealed that these aggregates were not sufficient to challenge BLM formation.

To evaluate the surface energy of silane-modified surfaces, sessile droplet H_2O contact angles were measured on planar Si substrates (Supporting Information, Figure S3). Figure 2 summarizes the H_2O contact angles, *n*-decane contact angles, and surface energies of the silane modifiers used in this work.

Surface energy was calculated using the Young–Dupré–Good–Girifalco equation.[43−45]

$$\cos\theta = 2\phi\sqrt{\gamma_{sv}/\gamma_{lv}} - 1 \quad (1)$$

where ϕ is a correction factor (assumed here to be unity) and γ_{sv} and γ_{lv} are the interfacial free energies of solid–vapor and liquid–vapor interfaces, respectively. Using γ_{lv} = 72.8 mJ m^{-2} for a H_2O/atmosphere interface at 21.5 °C,[46] the surface energy was calculated for each modified substrate.

The static H_2O contact angles for PFDDCS, PFDCS, and CPDCS modifications agree well with previous reports.[47,40,48] Acid cleaned substrates appeared thoroughly wetted; thus, the H_2O contact angle was <10°. A minimum surface energy of 7.1 ± 2 mJ m^{-2} was achieved by functionalizing the high-energy surface of Si substrates with PFDDCS (contact angle = 113 ± 2°), agreeing well with previous reports for CF_3-modified surfaces.[49,50] Control surfaces treated with ACN or toluene showed only a small change in water contact angle (< 40°) compared to acid cleaned substrates, suggesting that the dominant influence on surface energy under these conditions was surface silane modification. Surface modifications that yielded the lowest surface energies, EDCS, ODCS, PFDCS, PFTCS, and PFDDCS, were selected for further investigation of BLM formation.

Contact angles of *n*-decane droplets were also measured to investigate the amphiphobicity of silane modifications, since amphiphobicity may have an impact on the formation of BLMs on modified surfaces. Following BLM painting, residual *n*-decane existing between monolayer leaflets and at BLM/support interfaces improves BLM stability by serving as a vibration absorber; however, excessive solvent layer thickness may increase electrical fluctuations during recordings[51] and challenge BLM formation. Solvent expulsion, or thinning, facilitates interactions between lipid tails and substrate surfaces.[30] On surfaces that are completely wetted by *n*-decane, membrane thinning may be much slower. Thus, surfaces that are selective to lipid/substrate over solvent/substrate interactions are preferred.

The *n*-decane contact angle measured on bare Si and on all modified substrates showed complete wettability (<10°) with the exception of PFDCS-, PFTCS-, and PFDDCS-modified substrates, which yielded contact angles of 52 ± 2, 63 ± 3, and 66 ± 3°, respectively. (Figure 2). Although the numbers of fluorocarbons for PFDCS and PFTCS were the same, the *n*-decane contact angles were statistically different. The higher *n*-decane contact angle for PFTCS is likely due to increased surface roughness following polymerization of the PFTCS. The complete wetting of bare Si and the hydrophobic modified substrate may be due to the dominant long-range van der Waals forces between bulk *n*-decane and the underlying Si.[52,53] The observed amphiphobic character of PFDCS-, PFTCS-, and PFDDCS-modified surfaces agrees well with previous reports[51] and may be particularly advantageous for BLM formation, as poorer solvent (e.g., *n*-decane) wetting may lead to more rapid thinning and more direct contact between the lipids and the aperture substrate.

Previous characterizations of lipid monolayers on modified substrates by fluorescence microscopy revealed that lipids exhibit a tail-down orientation to form lipid monolayers when vesicles were fused on CPDCS-modified planar glass substrates.[25,35,53] We followed a similar approach to evaluate membrane structure on the surface modifications investigated here. Complete fusion of lipid vesicles on unmodified or high energy surfaces was observed after ca. 30 min; however, vesicle fusion on low energy surfaces required longer fusion times (ca. 4–8 h), agreeing well with previous reports.[54−56,41] The surface was scratched to remove lipids, producing a fluorescence contrast, and a line profile of relative fluorescence intensity drawn from the scratched area to the lipid layer was used to determine the difference in lipid layer thickness. Cremer et al. have shown that scratching removes the underlying lipid layer, while permanent scoring of the lipid layer was pH dependent. Thus, at basic pH, the scratch was permanent but would heal at a lower pH (4.5).[35]

The formation of hybrid lipid membranes on low energy PFDCS- and PFDDCS-modified surfaces compared to unmodified glass agrees well with prior reports[54−56] (Supporting Information, Figure S4). Table 2 shows normalized fluorescence intensities for membranes deposited on silane-modified surfaces. Fluorescence intensities of the lipid layer on all silane-modified glass substrates were ca. 50% that of unmodified glass, which is well-established to support lipid bilayers, supporting the presence of a lipid monolayer formed due to lipid tail/substrate interactions. All of the selected modified surfaces supported lipid monolayer formation within 4–8 h of vesicle fusion except PFTCS-modified surfaces. The normalized fluorescence intensity of lipid membrane on PFTCS corresponded to less than half a bilayer (0.35 ± 0.11) due to the heterogeneous surface of PFTCS-modified substrates, which had a significant influence on membrane deposition (Supporting Information, Figure S4). The adverse effect of heterogeneous substrates on uniform lipid monolayer membrane formation agrees with previous work.[55,57]

Table 2. Normalized Fluorescence Intensities of DLPC/Rh-DPPE Layers on Silane-Modified Surfaces

modifier	normalized intensity[a]
none (control)	0.96 ± 0.03
CPDCS	0.51 ± 0.02
EDCS	0.48 ± 0.02
ODCS	0.50 ± 0.02
PFDCS	0.52 ± 0.02
PFTCS	0.35 ± 0.11
PFDDCS	0.45 ± 0.08

[a]8 h fusion time.

Although complete vesicle fusion occurred after ca. 10 h, defects were still present for PFTCS-modified substrates. The normalized fluorescence intensity of the lipid monolayer membrane, however, increased by 31% from 0.35 ± 0.11 in 8 h to 0.44 ± 0.04 in ca. 10 h for regions that supported hybrid bilayer formation. Conversely, increased time of vesicle fusion on PFDDCS-modified substrate resulted in complete hybrid lipid membrane formation (0.51 ± 0.06) with no observable defects. While vesicle fusion on high energy surfaces involves adsorption, rapture, and fusion, the mechanism of vesicle disruption on low energy surfaces is unknown.[58] Although the rate of vesicle fusion leading to monolayer membrane formation is slowed on very low energy surfaces,[54] the mechanism differs for BLM formation across modified pipette apertures which requires manual painting and solvent thinning.

Pipette Aperture Characterization. Following the identification of suitable surface conditions to form uniform lipid monolayers on silane-modified planar surfaces, we directly

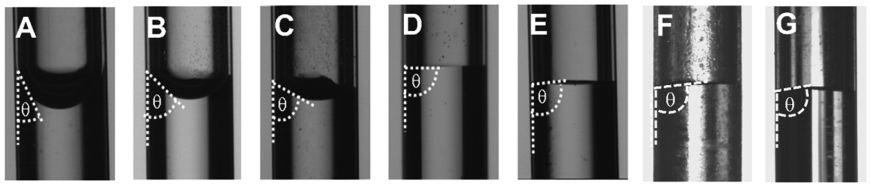

Figure 3. Estimation of H_2O contact angle in 1.1 mm I.D. capillaries. The capillaries were (A) acid cleaned, (B) CPDCS-modified, (C) EDCS-modified, (D) ODCS-modified, (E) PFDCS-modified, (F) PFTCS-modified, and (G) PFDDCS-modified.

Table 3. Physical and Electrical Properties of BLMs Suspended on Silane-Modified Pipette Apertures

modifier	surface energy (mJ m^{-2})	V_B (mV)	air−water transfer	normalized conductance ($\times 10^{-2}$ pS μm^{-2})	longevity (h)
unmodified	68 ± 0.5	N.A.[a]	1	17.2 ± 2.4	0.6 ± 0.3
CPDCS	54 ± 2.0	418 ± 73	2.0 ± 0.2	5.8 ± 0.5	2 ± 1
EDCS	40 ± 0.8	525 ± 34	4.8 ± 1	4.7 ± 1.4	3 ± 1
ODCS	18 ± 0.4	605 ± 53	6.1 ± 2	2.4 ± 0.7	6 ± 2
PFDCS	16 ± 1.0	885 ± 62	>50	8.3 ± 3.3	8 ± 1
PFDDCS	11 ± 1.0	>2000[b]	>50	6.1 ± 1.2	>13
PFTCS	16 ± 0.9	N.A.[a]	N.A.[a]	N.A.[a]	N.A.[a]

[a]N.A.: not available due to frequent clogging. [b]No breakdown, transient pores observed at 2000 mV.

evaluated the effects of silane composition on pipette surface chemistry and BLM formation. Direct surface characterization of glass micropipet apertures is challenging due to the surface topology; thus, different, but complementary, characterization methods were employed.

To evaluate the surface energy of the apertures, glass capillaries from which pipette apertures are fabricated were modified with CPDCS, EDCS, ODCS, PFDCS, PFTCS, or PFDDCS. APDCS, FPDCS, and TCS were excluded from further study due to the high surface energies observed. The interfacial free energies for the solid−vapor interfaces were qualitatively distinguished by capillary action, as shown in Figure 3. The hydrophobicity in the modified glass pipettes increased (CPDCS < EDCS < ODCS < PFDCS = PFTCS < PFDDCS), as indicated by increasing H_2O contact angles of 44 ± 2, 61 ± 1, 90 ± 1, 93 ± 2, 94 ± 2, and 101 ± 3°, respectively. Surface free energy (γ) for the solid−liquid interface was calculated for each condition based on eq 2

$$\gamma = \frac{\rho g r h}{2 \cos \Theta} \tag{2}$$

where h is the equilibrium water rise height, Θ is the contact angle of the surface, r is the capillary radius, g is the gravitational constant, and ρ is the density of water.[59] The high surface energy of unmodified glass pipettes (68 ± 0.5 mJ m^{-2}) was markedly reduced after modification with selected silane modifiers (Table 3). Surface energies ranging from 11 to 54 mJ m^{-2} were measured for the silane modifiers investigated, with the lowest surface energies corresponding to the perfluorinated modified surfaces. Although the estimated surface energies in modified capillaries were higher than those observed on planar substrates, the decreasing trend in surface energy (Table 3) was similar, indicating that the silane modification protocol was suitable for modification of glass micropipet apertures.

We then explored the relationship between silane modifier composition and BLM stability. BLMs were formed across modified micropipet apertures of 25−35 μm diameter, and membrane conductance, breakdown voltage (V_B), longevity, and the number of air−water transfers (AWT) were measured as indicators of BLM stability. Membrane conductance and V_B are complementary measures of electrical stability, while AWT and longevity are metrics of mechanical and temporal stability, respectively.

We observed rapid (<2 min) formation of BLMs across PFDCS- and PFDDCS-modified apertures, which may be due to the rapid exclusion of residual *n*-decane from the monolayer leaflets and at the BLM/support interface. Exclusion of *n*-decane from BLMs suspended across CPDCS-, EDCS-, and ODCS-modified pipettes was slower and thus required 5−10 min to reach stable recordings, when monitored by conductance curves. Though fusion to hydrophobic substrates, including the amphiphobic modifiers PFDCS and PFDDCS, was slowed substantially, the mechanism of BLM formation is quite different, which accounts for the more rapid BLM formation observed. Vesicle fusion relies on vesicle size, concentration, and intermolecular forces that lead to interaction and rupture of the vesicle on the substrate.[55] Conversely, BLM formation relies on manual painting, lipid organization, and subsequent thinning of residual organic solvent trapped between the leaflets of the bilayer. In surfaces that are well wetted by organic solvents, thinning is slowed compared to amphiphobic surfaces that better exclude these solvents.

Increased interaction between the lipid and the modified aperture surfaces should result in decreased ion conductance at the lipid−aperture interface. All modifiers used in the present study, except PFTCS, were capable of supporting BLM formation and exhibited statistically significant reductions in leakage currents relative to unmodified glass pipettes (Table 3). Despite a low surface energy, we were unable to form BLMs using PFTCS, likely due to the increased surface roughness and silane aggregation observed on planar substrates. ODCS-modified pipettes yielded a two-fold reduction in mean BLM conductance compared with CPDCS-modified pipettes, with conductances of $(2.4 \pm 0.7) \times 10^{-2}$ and $(5.8 \pm 0.5) \times 10^{-2}$ pS μm^{-2}, respectively. BLM conductance for EDCS-modified pipettes was not statistically different from CPDCS-modified pipettes with 95% confidence. Interestingly, BLM conductance on PFDCS- and PFDDCS-modified pipettes ($(8.3 \pm 3.3) \times 10^{-2}$ and $(6.1 \pm 1.2) \times 10^{-2}$ pS μm^{-2}, respectively) was similar to CPDCS-modified pipettes. The increased conductance for PFDCS and PFDDCS relative to ODCS, which exhibits a

similar surface energy to PFDCS, may result from a combination of two possible phenomena. First, silane aggregates observed in AFM images of the PFDCS-modified substrates (Supporting Information, Figure S2) may contribute to a poor electrical seal at the aperture−membrane interface, though not inhibit BLM formation. Second, the amphiphobic property of PFDCS and PFDDCS modification may result in decreased annulus volume at the aperture−membrane interface, which would effectively increase the active area of the lipid bilayer, leading to increased total conductance. The latter phenomenon is further supported by studies performed on the process of BLM formation which is dependent on solvent thinning across preconditioned apertures.[30,51] Snyder et al. showed that BLM formation starts by expelling solvent from lipid monolayer leaflets into the annulus region. Thus, the less solvent that exists between lipid monolayer leaflets, the faster the thinning rate and the larger the active area of BLM formed.[60] In this study, bilayer area was assumed to be unaffected by surface modifications, which may have introduced systematic bias in the area-normalized conductance values.

V_B represents the potential at which a large, nonlinear increase in ion conductance is observed, resulting from electrical breakdown of the lipid bilayer. Thus, V_B provides an indication of the electrical stability of the BLM. The observed V_B for DPhPC bilayers suspended across CPDCS-modified apertures (418 ± 73 mV) agreed well with previous reports.[61] For DPhPC BLMs suspended across CPDCS-, EDCS-, ODCS-, PFDCS-, and PFDDCS-modified pipette apertures, BLM breakdown was observed to increase with decreasing surface energy (Table 3), indicating that increased interaction between lipid tails and modified surfaces leads to improved electrical stability. Bilayer breakdown can be classified as either irreversible or reversible, based on whether the bilayer reforms spontaneously (reversible) or not (irreversible).[62,63] BLMs formed on ODCS-, PFDCS-, and PFDDCS-modified pipettes underwent reversible breakdown, whereas BLMs suspended on CPDCS- and EDCS-modified pipettes underwent irreversible breakdown. The reversible breakdown of BLMs on low energy surfaces may suggest that the mechanism of breakdown is affected by increased lipid−surface interactions at the bilayer−aperture interface, though investigation of the underlying phenomenon is beyond the scope of this work.

AWT refers to the number of times a bilayer survives transport across an air−water interface, and provides an indication of the relative mechanical stability of the BLMs, since synthetic lipid membranes readily degrade when exposed to air. As seen in Table 3, silane modification markedly increased the mechanical stability of the BLM. Interestingly, this effect is substantially higher for PFDCS and PFDDCS compared to other silanes. The observed increase in the number of air−water transfer measurements may be due to a stronger intercalation between the hydrophobic tail of the lipid monolayer and the underlying hydrophobic or amphiphobic substrate.

BLM lifetime is measured as the average time required for a BLM to spontaneously break down under the application of a ±5 mV 20 Hz square-wave test pulse. Decreased surface energy clearly resulted in increased temporal stability, with average lifetimes of 6 to >13 h observed for BLMs on ODCS-, PFDCS-, and PFDDCS-modified apertures compared to 2 ± 1 h for CPDCS-modified and 0.6 ± 0.3 h for unmodified apertures. The increase in average lifetime likely results from the stronger interactions between the lipid and the underlying surfaces, minimizing gradual surface dissociation of lipids, which ultimately leads to catastrophic breakdown.

Overall, improved electrical, mechanical, and temporal stability of BLMs suspended across silane-modified apertures was strongly correlated with decreasing aperture surface energy. We attribute this correlation to increased interactions between lipid tails and the silane-modified aperture surface, which acts to anchor the BLM to the aperture. Interestingly, increased BLM stability may not be strictly the result of decreased surface energy but in the case of PFDCS- or PFDDCS-modified apertures may also benefit from selective lipid−substrate interactions. PFDCS and PFDDCS were unique among the surface modifiers for their amphiphobic quality, which resists wetting by either H_2O or *n*-decane (Figure 2). Previous reports have shown perfluorinated surfaces are slightly wetted by lipids.[28,54] While the present work did not study the wettability of modified surfaces by lipids, it is likely that lipid/substrate interactions favored over *n*-decane/substrate interactions play a crucial role in the marked improvement of BLM stability observed on PFDCS- and PFDDCS-modified apertures.

Reconstitution of Ion Channel Forming Peptides. To ensure that the increased stability observed for silane-modified apertures did not negatively affect BLM fluidity and, thus, ion channel recordings, the bacterial protein (α-HL) was reconstituted into BLMs formed across apertures modified with varying silanes. α-HL forms a 26 Å diameter pore with a characteristic conductance of 1 nS,[64,65] and is commonly utilized for BLM characterization. Insertion of α-HL was evaluated by monitoring the ion current across the BLM. Reconstitution of α-HL into the BLM was observed as a step increase in current of approximately 40 pA (Supporting Information, Figure S5), at which time bath solution was immediately diluted to prevent multiple ion channel insertions. Table 4 summarizes the mean conductance measured upon reconstitution of α-HL into BLMs supported on silane-modified apertures. The α-HL conductance in each case (ca. 1 nS) agrees well with previous reports,[65] and no statistically unique populations were observed (Supporting Information, Figure S5). α-HL reconstitution clearly demonstrated that stabilized BLMs formed on silane-modified pipette apertures exert no negative impact on ion channel activity. Interestingly, a decrease in baseline noise was observed that corresponded to decreased surface energy. This phenomenon is likely due to decreasing dielectric properties of the apertures which are similar to low-noise recordings observed for BLMs suspended across highly hydrophobic Teflon apertures.[66] Although ODCS BLMs yielded an ca. 2−4-fold reduction in the magnitude of ion conductance background compared to PFDCS- and PFDDCS-modified apertures, the reduced baseline noise generated by PFDCS or PFDDCS modification may offset this difference for future sensor measurements.

Table 4. α-HL Conductance in BLMs Suspended from Silane-Modified Glass Apertures

modifier	α-HL conductance (nS)
CPDCS	0.93 ± 0.11
EDCS	0.83 ± 0.23
ODCS	1.03 ± 0.05
PFDCS	1.00 ± 0.08
PFDDCS	0.92 ± 0.06

CONCLUSIONS

This study addressed a key requirement for long-term, widespread realization of ion-channel-functionalized sensors—increased membrane stability. Surface-modified planar Si substrates were investigated to identify substrate modifications that lead to highly stable BLMs for long term recordings. Low energy surfaces were found to provide markedly enhanced BLMs with respect to electrical, mechanical, and temporal stability while supporting lower noise ion channel recordings. Of particular interest, modification with perfluorinated silane modifiers, PFDCS and PFDDCS, afforded a 4- to 7-fold increase in BLM lifetime, a 2- to 5-fold increase in electrical stability, and a >25-fold increase in mechanical stability when compared to conventional (CPDCS) modifications. This approach is simple, low cost, and widely accessible, suggesting that it could immediately impact the development of ion-channel-functionalized sensors and other techniques that rely upon the formation of stabilized lipid bilayers across micrometer-sized apertures.

ASSOCIATED CONTENT

Supporting Information

Additional data figures as indicated in the text, including additional surface characterization and ion channel recordings. This material is available free of charge via the Internet at http://pubs.acs.org.

AUTHOR INFORMATION

Corresponding Author

*Address: Department of Chemistry and Biochemistry, University of Arizona, 1306 E. University Blvd, Tucson, AZ 85721. Phone: 520-621-6338. Fax: 520-621-8407. E-mail: aspinwal@email.arizona.edu.

Notes

The authors declare no competing financial interest.

ACKNOWLEDGMENTS

This work was supported in part by the National Institutes of Health under Grant Nos. GM095763 and EB007047. L.M. was supported via the Undergraduate Biology Research Program at the University of Arizona under Grant No. HHMI 52006942.

REFERENCES

(1) Lathrop, D. K.; Ervin, E. N.; Barrall, G. A.; Keehan, M. G.; Kawano, R.; Krupka, M. A.; White, H. S.; Hibbs, A. H. *J. Am. Chem. Soc.* **2010**, *132*, 1878−1885.
(2) Branton, D.; Deamer, D. W.; Marziali, A.; Bayley, H.; Benner, S. A.; Butler, T.; Di Ventra, M.; Garaj, S.; Hibbs, A.; Huang, X. *Nat. Biotechnol.* **2008**, *26*, 1146−1153.
(3) Kasianowicz, J. J.; Robertson, J. W. F.; Chan, E. R.; Reiner, J. E.; Stanford, V. M. *Annu. Rev. Anal. Chem.* **2008**, *1*, 737−766.
(4) Aoki, H.; Bühlmann, P.; Umezawa, Y. *Electroanalysis* **2000**, *12*, 1272−1276.
(5) Howorka, S.; Cheley, S.; Bayley, H. *Nat. Biotechnol.* **2001**, *19*, 636−639.
(6) Orwar, O.; Jardemark, K.; Jacobson, I.; Moscho, A.; Fishman, H. A.; Scheller, R. H.; Zare, R. N. *Science* **1996**, *272*, 1779−1782.
(7) Braha, O.; Gu, L. Q.; Zhou, L.; Lu, X. F.; Cheley, S.; Bayley, H. *Nat. Biotechnol.* **2000**, *18*, 1005−1007.
(8) Overington, J. P.; Al-Lazikani, B.; Hopkins, A. L. *Nat. Rev. Drug Discovery* **2006**, *5*, 993−996.
(9) Dunlop, J.; Bowlby, M.; Peri, R.; Vasilyev, D.; Arias, R. *Nat. Rev. Drug Discovery* **2008**, *7*, 358−368.
(10) Robertson, J. W. F.; Rodrigues, C. G.; Stanford, V. M.; Rubinson, K. A.; Krasilnikov, O. V.; Kasianowicz, J. J. *Proc. Natl. Acad. Sci. U.S.A.* **2007**, *104*, 8207−8211.
(11) Mueller, P.; Rudin, D. O.; Tien, H. T.; Wescott, W. C. *Nature* **1962**, *194*, 979−980.
(12) Hirano-Iwata, A.; Aoto, K.; Oshima, A.; Taira, T.; Yamaguchi, R.-t.; Kimura, Y.; Niwano, M. *Langmuir* **2010**, *26*, 1949−1952.
(13) Hirano-Iwata, A.; Oshima, A.; Nasu, T.; Taira, T.; Kimura, Y.; Niwano, M. *Supramol. Chem.* **2010**, *22*, 406−412.
(14) Maurer, J. A.; White, V. E.; Dougherty, D. A.; Nadeau, J. L. *Biosens. Bioelectron.* **2007**, *22*, 2577−2584.
(15) Kang, X. F.; Cheley, S.; Rice-Ficht, A. C.; Bayley, H. *J. Am. Chem. Soc.* **2007**, *129*, 4701−4705.
(16) Jeon, T. J.; Malmstadt, N.; Schmidt, J. J. *J. Am. Chem. Soc.* **2006**, *128*, 42−43.
(17) Benz, R.; Elbert, R.; Prass, W.; Ringsdorf, H. *Eur. Biophys. J.* **1986**, *14*, 83−92.
(18) Heitz, B. A.; Xu, J.; Jones, I. W.; Keogh, J. P.; Comi, T. J.; Hall, H. K., Jr.; Aspinwall, C. A.; Saavedra, S. S. *Langmuir* **2011**, *27*, 1882−1890.
(19) Zhang, H.; Joubert, J. R.; Saavedra, S. S. *Adv. Polym. Sci.* **2010**, *224*, 1−42.
(20) Heitz, B. A.; Jones, I. W.; Hall, H. K.; Aspinwall, C. A.; Saavedra, S. S. *J. Am. Chem. Soc.* **2010**, *132*, 7086−7093.
(21) Malmstadt, N.; Jeon, T. J.; Schmidt, J. J. *Adv. Mater.* **2008**, *20*, 84−89.
(22) Ahl, P. L.; Price, R.; Smuda, J.; Gaber, B. P.; Singh, A. *Biochim. Biophys. Acta* **1990**, *1028*, 141−153.
(23) Mueller, A.; O'Brien, D. F. *Chem. Rev.* **2002**, *102*, 727−758.
(24) White, R. J.; Zhang, B.; Daniel, S.; Tang, J. M.; Ervin, E. N.; Cremer, P. S.; White, H. S. *Langmuir* **2006**, *22*, 10777−10783.
(25) Krishna, G.; Schulte, J.; Cornell, B. A.; Pace, R. J.; Osman, P. D. *Langmuir* **2003**, *19*, 2294−2305.
(26) White, R. J.; Ervin, E. N.; Yang, T.; Chen, X.; Daniel, S.; Cremer, P. S.; White, H. S. *J. Am. Chem. Soc.* **2007**, *129*, 11766−11775.
(27) Oshima, A.; Hirano-Iwata, A.; Mozumi, H.; Ishinari, Y.; Kimura, Y.; Niwano, M. *Anal. Chem.* **2013**, *85*, 4363−4369.
(28) Plant, A. L. *Langmuir* **1999**, *15*, 5128−5135.
(29) Montal, M.; Mueller, P. *Proc. Natl. Acad. Sci. U.S.A.* **1972**, *69*, 3561−3566.
(30) Kremer, J. M. H.; Agterof, W. G. M.; Wiersema, P. H. *J. Colloid Interface Sci.* **1977**, *62*, 396−405.
(31) Heitz, B. A.; Xu, J.; Hall, H. K., Jr.; Aspinwall, C. A.; Saavedra, S. S. *J. Am. Chem. Soc.* **2009**, *131*, 6662−3.
(32) White, S.; Petersen, D.; Simon, S.; Yafuso, M. *Biophys. J.* **1976**, *16*, 481−489.
(33) Pantoja, R.; Sigg, D.; Blunck, R.; Bezanilla, F.; Heath, J. R. *Biophys. J.* **2001**, *81*, 2389−2394.
(34) Ross, E. E.; Rozanski, L. J.; Spratt, T.; Liu, S. C.; O'Brien, D. F.; Saavedra, S. S. *Langmuir* **2003**, *19*, 1752−1765.
(35) Cremer, P. S.; Groves, J. T.; Kung, L. A.; Boxer, S. G. *Langmuir* **1999**, *15*, 3893−3896.
(36) Abramoff, M. D.; Magalhaes, P. J.; Ram, S. J. *Biophotonics Int.* **2004**, *11*, 36−42.
(37) Van Der Voort, P.; Vansant, E. F. *J. Liq. Chromatogr. Relat. Technol.* **1996**, *19*, 2723−2752.
(38) Halliwell, C. M.; Cass, A. E. G. *Anal. Chem.* **2001**, *73*, 2476−2483.
(39) Schibel, A. E. P.; Edwards, T.; Kawano, R.; Lan, W.; White, H. S. *Anal. Chem.* **2010**, *82*, 7259−7266.
(40) Falipou, S.; Chovelon, J. M.; Martelet, C.; Margonari, J.; Cathignol, D. *Sens. Actuators, A* **1999**, *74*, 81−85.
(41) Ratnayaka, S. N.; Wysocki, R. J., Jr.; Saavedra, S. S. *J. Colloid Interface Sci.* **2008**, *327*, 63−74.
(42) Miwa, M.; Nakajima, A.; Fujishima, A.; Hashimoto, K.; Watanabe, T. *Langmuir* **2000**, *16*, 5754−5760.
(43) Nakajima, A. *NPG Asia Mater.* **2011**, *3*, 49−56.
(44) Girifalco, L.; Good, R. *J. Phys. Chem.* **1957**, *61*, 904−909.
(45) Chaudhury, M. K. *Mater. Sci. Eng. Rep.* **1996**, *16*, 97−159.

(46) Phang, T. L.; Franses, E. I. *Langmuir* **2006**, *22*, 1609−1618.
(47) Kasai, T.; Bhushan, B.; Kulik, G.; Barbieri, L.; Hoffmann, P. *J. Vac. Sci. Technol., B* **2005**, *23*, 995−1003.
(48) Hozumi, A.; Ushiyama, K.; Sugimura, H.; Takai, O. *Langmuir* **1999**, *15*, 7600−7604.
(49) Nishino, T.; Meguro, M.; Nakamae, K.; Matsushita, M.; Ueda, Y. *Langmuir* **1999**, *15*, 4321−4323.
(50) Shafrin, E. G.; Zisman, W. A. *J. Phys. Chem.* **1960**, *64*, 519−524.
(51) Batishchev, O. V.; Indenbom, A. V. *Bioelectrochemistry* **2008**, *74*, 22−25.
(52) Quéré, D. *Phys. A (Amsterdam, Neth.)* **2002**, *313*, 32−46.
(53) Ingram, B. T. *J. Chem. Soc., Faraday Trans. 1* **1974**, *70*, 868−876.
(54) Silin, V. I.; Wieder, H.; Woodward, J. T.; Valincius, G.; Offenhausser, A.; Plant, A. L. *J. Am. Chem. Soc.* **2002**, *124*, 14676−14683.
(55) Hubbard, J. B.; Silin, V.; Plant, A. L. *Biophys. Chem.* **1998**, *75*, 163−176.
(56) Plant, A. L. *Langmuir* **1993**, *9*, 2764−2767.
(57) Seu, K. J.; Pandey, A. P.; Haque, F.; Proctor, E. A.; Ribbe, A. E.; Hovis, J. S. *Biophys. J.* **2007**, *92*, 2445−2450.
(58) Lingler, S.; Rubinstein, I.; Knoll, W.; Offenhäusser, A. *Langmuir* **1997**, *13*, 7085−7091.
(59) Adamson, A. W.; Gast, A. P. *Physical Chemistry of Surfaces*, 5th ed.; Wiley: New York, 1990; Vol. *4*, pp 4−18.
(60) Snyder, T. S.; Chiang, S. H.; Klinzing, G. E.; Tirio, A. P. *J. Colloid Interface Sci.* **1978**, *67*, 31−41.
(61) Diederich, A.; Strobel, M.; Meier, W.; Winterhalter, M. *J. Phys. Chem. B* **1999**, *103*, 1402−1407.
(62) Glaser, R. W.; Leikin, S. L.; Chernomordik, L. V.; Pastushenko, V. F.; Sokirko, A. I. *Biochim. Biophys. Acta* **1988**, *940*, 275−287.
(63) Klotz, K.-H.; Winterhalter, M.; Benz, R. *Biochim. Biophys. Acta* **1993**, *1147*, 161.
(64) Bayley, H.; Cremer, P. S. *Nature* **2001**, *413*, 226−230.
(65) Deamer, D. W.; Branton, D. *Acc. Chem. Res.* **2002**, *35*, 817−825.
(66) Mayer, M.; Kriebel, J. K.; Tosteson, M. T.; Whitesides, G. M. *Biophys. J.* **2003**, *85*, 2684−2695.